

AD No. 31658
ASTIA FILE COPY

PROGRESS REPORT
on
**INTERACTION OF ELECTRONS AND
R-F FIELDS**

By
W. G. WORCESTER
and
J. C. TWOMBLY

Technical Report No. 1

Covering the period
MARCH 1, 1953 - DECEMBER 1, 1953

PREPARED UNDER CONTRACT NO. 1147-01
FOR
OFFICE OF NAVAL RESEARCH

ENGINEERING EXPERIMENT STATION
UNIVERSITY OF COLORADO
BOULDER, COLORADO

THIS REPORT HAS BEEN DELIMITED
AND CLEARED FOR PUBLIC RELEASE
UNDER DOD DIRECTIVE 5200.20 AND
NO RESTRICTIONS ARE IMPOSED UPON
ITS USE AND DISCLOSURE.

DISTRIBUTION STATEMENT A

APPROVED FOR PUBLIC RELEASE;
DISTRIBUTION UNLIMITED.

ACKNOWLEDGEMENT

The research reported in this document was made possible through support extended to the Engineering Experiment Station, University of Colorado, by the Navy Department (Office of Naval Research) under ONR Contract No. 1147-01.

This work represents the joint effort of a number of people, and especially Professors H. B. Palmer and S. I. Pearson of the Electrical Engineering Staff; J. C. Twombly, Associate Research Engineer; S. G. Andresen, P. G. Baird, and L. O. Nippe, research assistants; and W. G. Worcester, Research Engineer.

The report covers the period from March 1, 1953 to November 30, 1953.

ABSTRACT

This report describes the measurements that have been made on a simple beam-tester tube, including preliminary noise measurements.

A method for calculating the sensitivity of a "honeycomb" grid as a detector is outlined, and some results of the calculations are given.

TABLE OF CONTENTS

	Page
LIST OF ILLUSTRATIONS	v
Chapter	
I. INTRODUCTION	1
II. CONSTRUCTION OF BEAM-TESTER TUBE	5
2.1 Tube Construction	5
2.2 Magnet Construction	7
III. STATIC CHARACTERISTICS OF BEAM-TESTER TUBE	8
3.1 Static Characteristics	3
3.2 The Fraction of Drift-Tube Current Which Reaches the Collector	14
IV. MEASUREMENT OF NOISE IN BEAM CURRENT	17
V. CALCULATION OF DETECTING GRID CHARACTERISTICS	21
5.1 Outline of Solution for Quiescent Condition	22
5.2 Experimental Results for the Quiescent Case	23
5.3 The Small Signal Case	25

LIST OF ILLUSTRATIONS

Figure	Page
1.1	1
3.1	10
3.2	11
3.3	13
3.4	14
3.5	16
4.1	18
5.1	24
5.2	26
5.3	27

CHAPTER I

INTRODUCTION

A considerable amount of work has been done, mostly at Stanford, on a tube that utilizes the cyclotron mode of interaction between electrons and r-f electric fields in the presence of a strong and uniform magnetic field. The interaction can best be described by reference to figure 1.1 below. Electrons emitted from the cathode

are accelerated by a low voltage so that they drift through the long anode, or drift tube. The drift tube also constitutes an r-f

structure, which may be a cavity, a wave-guide, or a parallel-strip line. An r-f electric field can thus

be applied at right angles to the d-c magnetic field. Electrons will tend to spiral about the magnetic flux lines with a natural

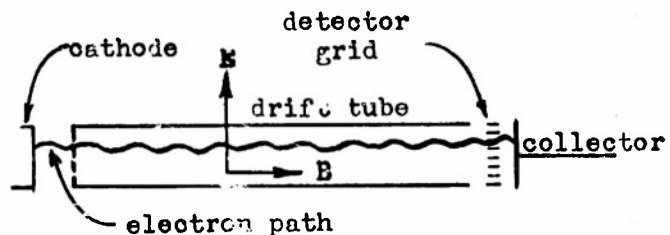


Fig. 1.1--Cyclotron-mode tube.

frequency, called the "cyclotron frequency", given by

$$f_0 = \frac{e}{2\pi m} B = 2.8 B \text{ mcps.}, \text{ where } (1-1)$$

B is in Gauss

If the applied r-f electric field has the same frequency, and the proper phase, a resonant condition will result, and the spiral path of the electrons will constantly increase in radius as the electron drifts across the tube. This change in radius can be detected by suitable grid structures located in the electron path, and the collector signal is a demodulated, or pulsating direct current. One may think of the tube, therefore, as a magnetically tuned radio receiver, complete except for amplification and indication of the signal.

The object of the project is to learn more about the mechanism of interaction between electrons and r-f fields, and to find improved means of detecting this interaction, with a view to increasing the sensitivity of devices that utilize this principle.

The procedure to be followed in carrying out the research is indicated by the following discussion.

Previous work has indicated that the noise carried by the electron stream is, at least under certain conditions, much lower than would be predicted on the basis of the usual equations for noise. However, there are several conditions in this device that are not the usual conditions in electron tubes. The electron velocity is exceptionally low. Cathode-anode voltage is of the

order of 2 volts, and the electrons drift for a relatively long period of time between closely-spaced conducting plates. Hence space-charge smoothing occurs between anode and cathode, and possibly also in the drift space. A theoretical evaluation of the smoothing effect of the space charge should be possible, and this should be confirmed by experimental methods. Preliminary results will be reported in chapter IV of this report.

It is known that triodes, tetrodes, etc. have higher noise than diodes because of "partition" effects. However, there are indications that the noise in the cyclotron-mode tube is less than would be predicted by known theories of partitioning. This should be investigated more carefully than has been done to date.

There are simple geometrical explanations of the behavior of detectors (grids) that are of simple geometric form. Such explanations are reasonably satisfactory for the large-signal case, but we are not much interested in this case. For small signals, it is necessary to take into account the distribution of initial electron velocities transverse to the magnetic field, and the problem immediately becomes more involved. Also, the effect of d-c fields adjacent to the detector, and resulting from space-charge potentials, needs to be explored. It should be feasible to analyze the performance of a number of types of grid, and those that appear to be the most promising can be checked experimentally.

Under certain conditions of cathode temperature, magnetic field strength, anode voltage, and collector bias, both oscillations and

increased noise have been observed. There is a strong suspicion that the space-charge smoothing of the beam may be lost, giving rise to increased noise. The oscillations may also be caused by the pressure of gases in the tube. Complete evaluation of this effect is needed.

It has been suggested that the signal strength could be enhanced by using a secondary electron multiplier between the detector and the collector. No work has been done towards applying this scheme, but it deserves careful evaluation.

There are at least two possible ways to cover a wide range of frequencies with the cyclotron-mode tube. A tube can be designed for each desired frequency range, within certain practical limitations, or the signal frequency can be converted by heterodyning to bring it within the frequency range of the tube. Both methods need to be evaluated with respect to practicability, sensitivity, and cost.

CHAPTER II

CONSTRUCTION OF BEAM-TESTER TUBE

The objectives outlined in the first chapter include measurement of beam noise, partition effects, and oscillations, all of which occur in the absence of radio-frequency fields. A simple tube has been constructed for use in investigating static characteristics and noise. No provision was made for the introduction of r-f power. Nevertheless, some conclusions can be drawn with regard to sensitivity of different detecting grids because electrons are emitted from the cathode with transverse components of velocity, giving rise to helical electron paths. Changing the magnetic field strength will change the radii of the electron paths, and such changes can be detected by suitable grid structures.

2.1 Tube Construction

The principle features of the beam-tester tube are shown clearly by figure 2.1. The tube is of metal and ceramic construction. Both ends are sealed with O-ring gaskets, so that the tube can easily be disassembled for modification of the cathode or grid assemblies. Both end plates are made of steel, and form part of the magnet structure.

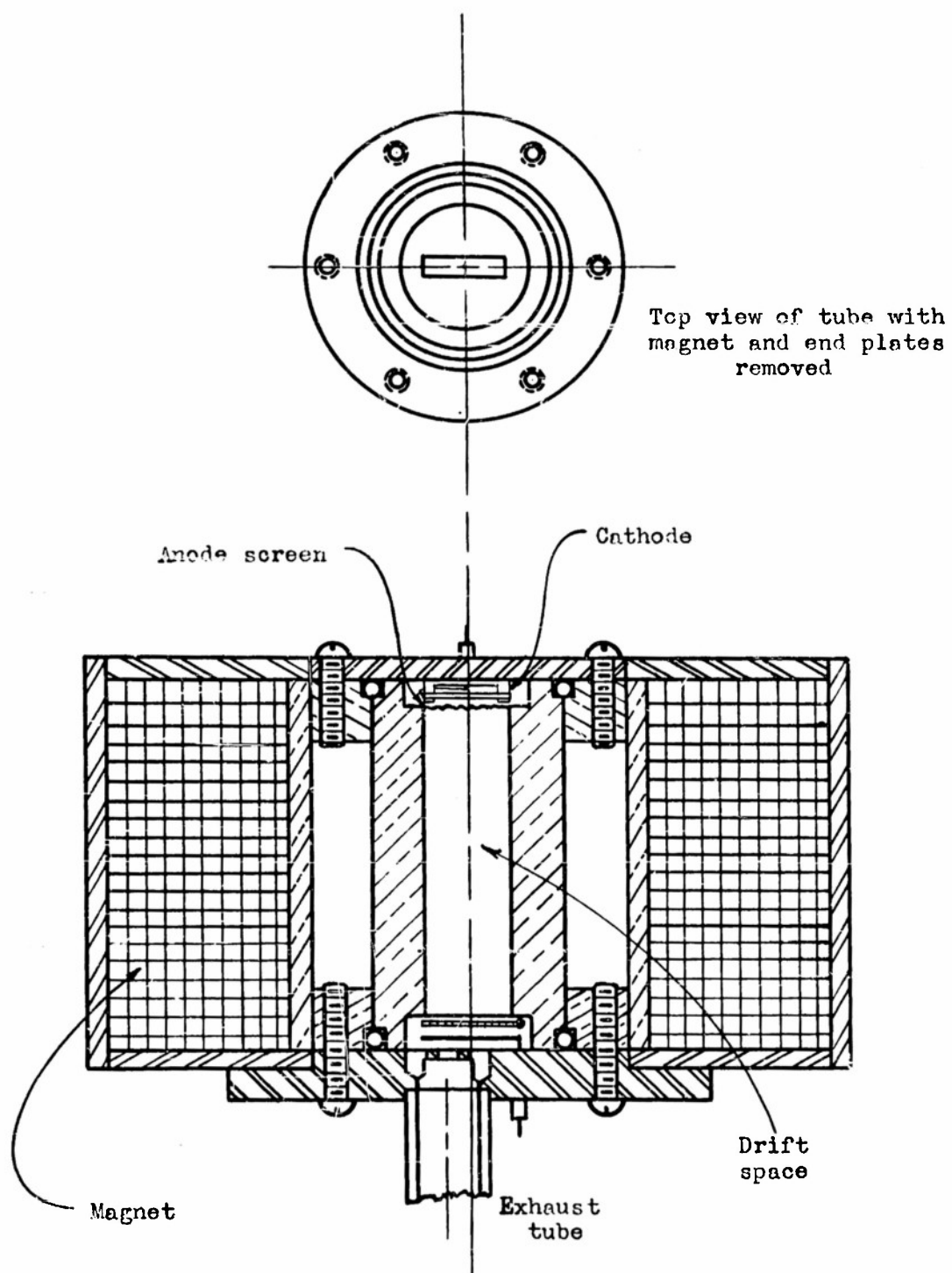


Fig. 2.1.--Diagram of experimental beam-tester tube.

The copper body of the tube was made in two halves and brazed together to provide a rectangular drift tube $1/8$ inch high, $1/2$ inch wide, and $1-7/8$ inches long. Copper flanges were brazed to the tube in the same operation.

The cathode and heater were taken from a type 6J6 tube and mounted in a holder machined from lava. The 6J6 cathode is flat, and has just the dimensions needed to cover the end of the drift tube.

An accelerating grid (or anode) was made by welding a fine tungsten screen (120 mesh, 0.0015 inch wire) to a molybdenum plate. Anode-cathode spacing was initially 0.025 inches, but the position of the grid can easily be changed. This will be done eventually as a means of determining the degree of space-charge saturation in the drift tube, and the effect thereof on beam noise.

A detecting grid was made by mounting three Varian klystron grids side-by-side. Overlapping portions of the circular grids were removed by slicing with a sharp razor blade, so that the grids formed essentially a continuous honeycomb structure covering the end of the drift tube, but insulated from it. The grids were mounted directly on a ceramic-metal seal, as was the collector plate. Thus it was possible to control the potential of each element, and measure grid and collector currents separately.

Insofar as it was possible, the dimensions of the beam-tester tube were chosen to correspond with those that would be used in a practical cyclotron resonance tube.

2.2 Magnet Construction

The construction of the magnet is shown by figure 2.1. To reduce leakage and produce a uniform magnetic field, the magnet winding is totally encased in steel of sufficient thickness that the magnetomotive force required for the steel is negligible. Therefore the total magnetomotive force produced by the winding appears across the air gap in the center. The winding consists of 5899 turns of #27 copper wire with silicone-fiber glass insulation. The winding was vacuum impregnated with Dow-Corning No. 996 insulating varnish. A number of thermocouples were imbedded in the winding so that the hot spot temperature could be determined. This was done in order to make available design data which should make possible the design of a smaller magnet. Complete data on the magnet will be given in a forthcoming report.

CHAPTER III

STATIC CHARACTERISTICS OF BEAM-TEST TUBE

Following is a discussion of the results obtained thus far in experiments performed on the cyclotron beam-tester tube. A description of this tube and an illustrative diagram have been presented in chapter II of this report. Most of the experimental investigation to date has been centered around this tube.

3.1 Static Characteristics

There are five parameters whose independent variation must be considered in describing the direct current or static characteristics of the beam-tester tube. These are: (1) heater voltage (cathode temperature); (2) anode screen voltage (voltage of drift tube with respect to cathode); (3) detecting grid voltage; (4) collector voltage; (5) magnetic field strength.

Heater Voltage. In conventional tube operation, anode voltages are so high that the velocity an electron attains in traversing the cathode-anode space is negligibly affected by initial velocity of emission of the electrons. Hence, space charge limited operation results in a relatively flat curve of cathode current versus heater

voltage. However, in the tube here treated, velocity of emission is in many cases comparable to the velocity due to accelerating fields. For the anode voltages from 1 to 6 volts used in this tube, absolute space charge limitation in the usual sense never exists. Space current may be limited to a value well below total emission current, but increasing the cathode temperature will increase the total space current transmitted by adding appreciably to the average velocity of the emitted electrons. Thus, to reproduce a given set of static characteristics, one should be able to control closely not only the heater voltage, but also the emitting efficiency of the cathode surface. The fact that this is almost impossible to do with precision, however, does not appreciably alter the character of the data obtained. It only changes the scale factor. One important exception to this statement is the effect on transverse velocity, and hence, collection of current on the detecting grid, which will be discussed later. Curves of total cathode current and current transmitted through the drift tube as functions of heater voltage appear in figure 3.1.

Anode Voltage. Under space charge limited conditions, total current through the drift tube is influenced by anode voltage (drift tube-to-cathode voltage) through one of two considerations: (1), the usual three-halves power law, which predicts space-charge limited current in an ideal planar diode,

$$I = 2.335 \times 10^{-6} \frac{A}{x^2} V^{3/2} \text{ amperes,} \quad (3-1)$$

where A is the effective cathode area, x is the anode-cathode spacing, and V is the anode-cathode voltage in volts; and (2), Haeff's formula¹

¹A. V. Haeff, "Space Charge Effects in Electron Beams", Proc. IRE, 27, 586-602, (1939)

$$I = 9.35 \times 10^{-6} \frac{M}{d} V^{3/2} F_m \text{ amperes,} \quad (3-2),$$

which predicts the space charge limited current that can be caused to flow parallel to two equipotential conducting planes separated by a distance d . The width of the current-carrying channel is w , and V

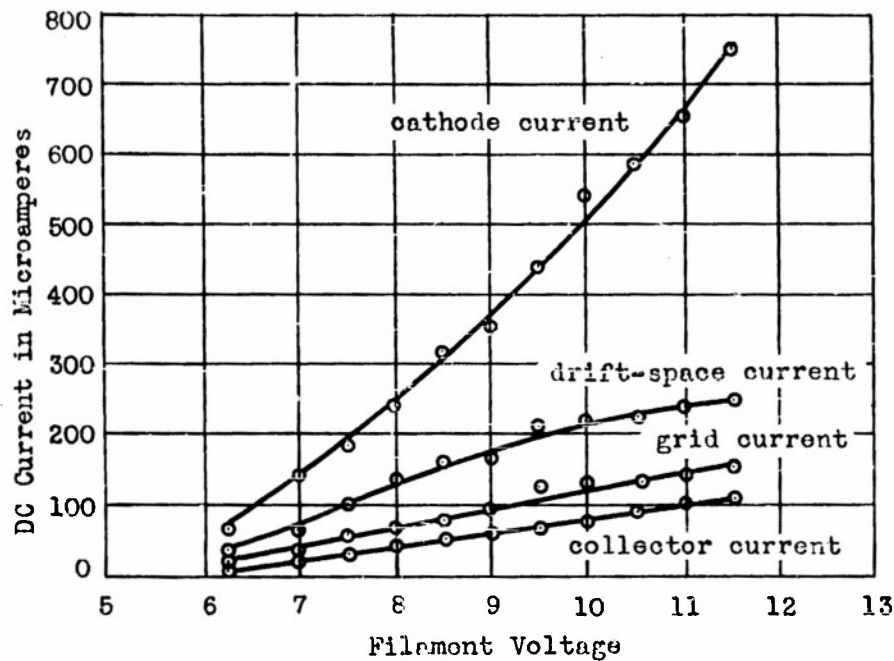


Fig. 3.1.--Beam-tester tube currents as functions of filament voltage.

is the accelerating voltage through which the electron passes before entering the space bounded by the conducting planes. The factor F_m has a value of 2.0 if the electron beam completely fills the space between the planes. Otherwise, it has a smaller value given by Haeff.

Drift-tube current is determined by the smaller of the two values predicted by the equations in the preceding paragraph. This tube is designed to give space charge limitation in the guide as predicted by Haeff's formula.

Thus, one would expect both the drift-tube current and total space current (drift-tube current plus current captured by the anode screen) to follow a $3/2$ -power variation with accelerating voltage. The total space current was found to follow this law, but drift-tube current variation exceeded the exponent $3/2$ at very low anode voltages (1.5 to 3 volts) and then returned to it for higher anode voltages. This variation, for a typical value of heater voltage, is shown in figure 3.2.

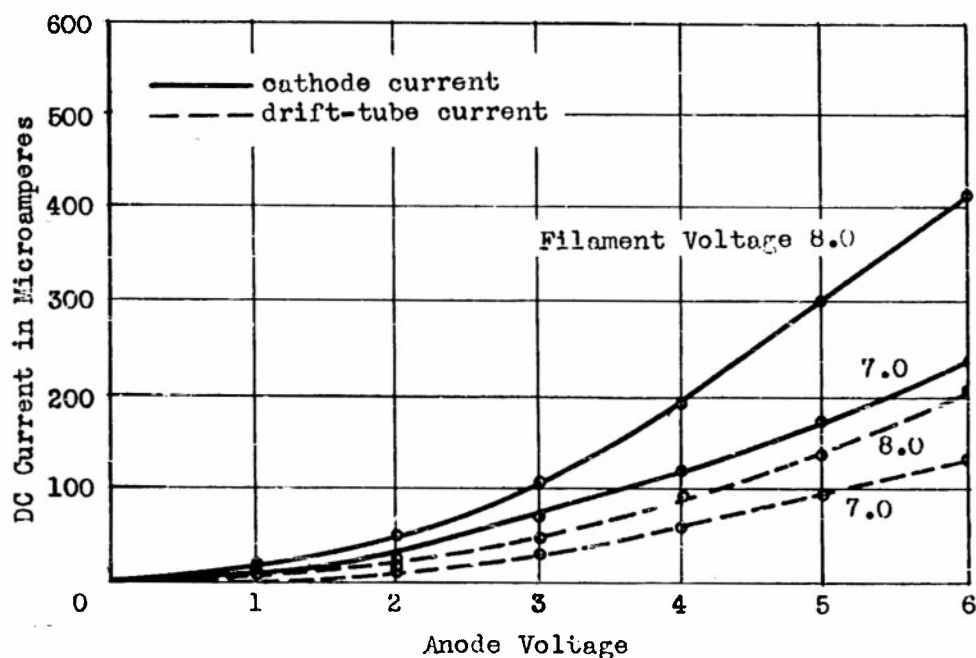


Fig. 3.2.--Beam-tester tube currents as functions of anode voltage.

Since 1.5 to 3.0 anode volts is the intended region of operation, efforts are being made to account for this discrepancy. Currently under investigation are two theories: (1), contact potentials; (2), contamination of the drift-tube walls by a thin oxide coating of appreciable resistivity. This latter possibility has been dealt with by gold

plating the copper tube body. Subsequent tests show more nearly proportional variation of the two currents with anode voltage, but the exponent is about 2 instead of $3/2$.

With the improved cathode emission obtained in recent tests, typical DC operating values are as follows:

Filament voltage:	7 volts
Anode voltage:	4 "
Detector grid voltage:	+ $1\frac{1}{2}$ " (with respect to drift tube)
Collector voltage:	+ $4\frac{1}{2}$ " " "
Total cathode emission:	325 microamperes
Drift-tube current:	135 "
Detector grid current:	55 "
Collector current:	85 "

Consistently, approximately 40 percent of the total cathode or total space current is transmitted through the drift tube. Capture by the anode grid and drift-tube walls account for the rest. From 50 percent to 70 percent of the drift-tube current normally reaches the collector, depending upon the factors which affect transverse electron velocity. These will be dealt with subsequently.

Detecting Grid Voltage. Figure 3.3 demonstrates that the grid voltage has little effect on any currents in the tube as long as the grid is at zero or positive voltage with respect to the tube body.

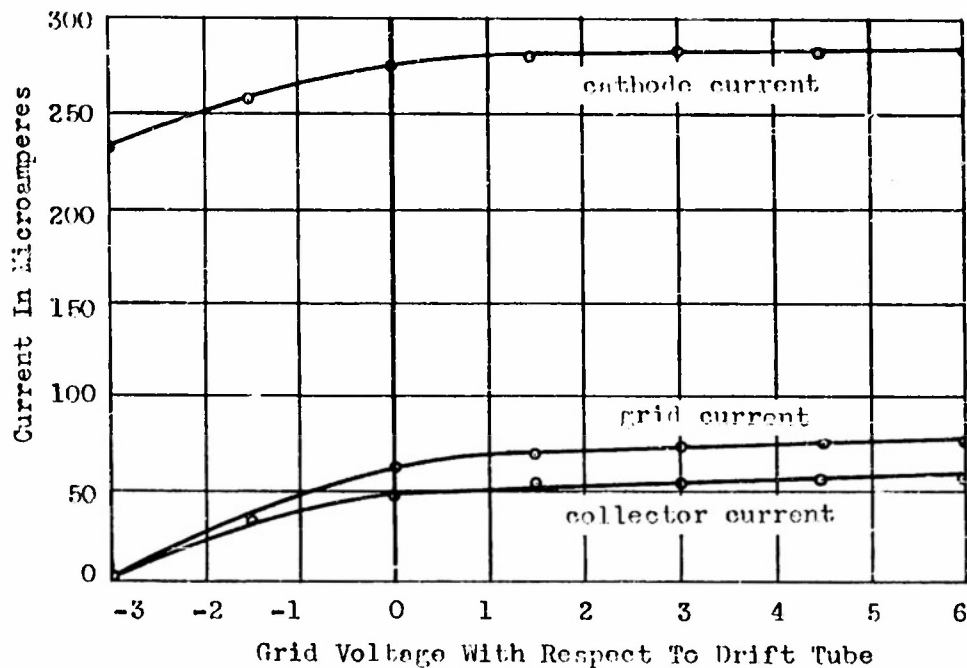


Fig. 3.5.--Beam-tester tube currents as functions of grid voltage.

Collector Voltage. Collector voltage was shown to have little effect on collector current as long as the collector is 2 volts or more positive with respect to the grid. This is evident in figure 3.4.

Magnet Current. The magnet current was found to have relatively little effect upon waveguide current as soon as the magnetic field exceeded the minimum value at which focusing begins. However, it was found to have the expected effect on the ratio of collector current to drift-tube current as treated in the next section.

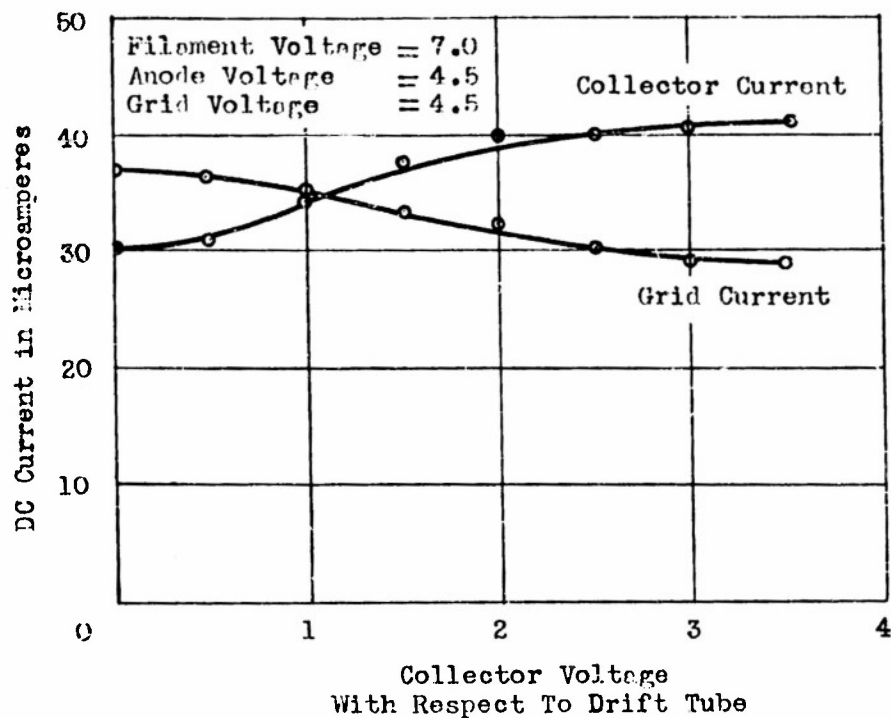


Fig. 3.4.--Collector current and grid current as functions of collector voltage.

3.2 The Fraction of Drift-Tube Current Which Reaches the Collector

The detecting action of the cyclotron-mode tube depends upon the fact that grids can be made to detect changes in the distribution of radii of the helical paths of electrons in a magnetic field. One theory which seems to fit the experimental data rather well, is outlined in chapter V of this report. Qualitatively, it is readily seen that a "honeycomb" grid structure, having a depth greater than the pitch of an electron path, will capture more electrons as the average radius is increased.

It should be emphasized at this point that there is no provision in the beam tester tube for introducing radio frequency fields; hence, the tube cannot be used for studies of cyclotron resonance. Nevertheless, individual electrons are emitted from the cathode with initial

transverse velocities, and therefore follow helical paths of the cyclotron frequency. Transverse electric fields in the neighborhood of the anode screen will alter the initial transverse velocity distribution.

Thus, of the independent variables in section A, anode voltage, heater voltage, and magnet current would be expected to influence the helix radius of electrons in the drift tube and, therefore, to influence the division of current between the "honeycomb" detecting grid and the collector.

Figure 3.5 shows the relative effects of anode voltage and magnetic field strength on the ratio of collector current to drift-tube current. The anode grid adds appreciably to transverse electron velocity as anode voltage is increased, as is evidenced by the increased capture of electrons by the grid at higher anode voltages. Since one of the primary objectives of this research is the reduction of transverse electron velocity not caused by the signal, inducement is added to the idea of arranging to do without the anode grid entirely. Schemes for doing this will therefore be evaluated in future experiments with this tube.

Cathode temperature was shown to have a negligible effect on transverse electron velocity at the collecting end of the drift tube. Changing the heater voltage from seven to nine volts made no apparent change in the ratio of collector current to drift-tube current. However, the ratio of collector current to cathode current decreased by about ten percent. This apparently shows that the drift-tube current is limited by space charge within the drift space.

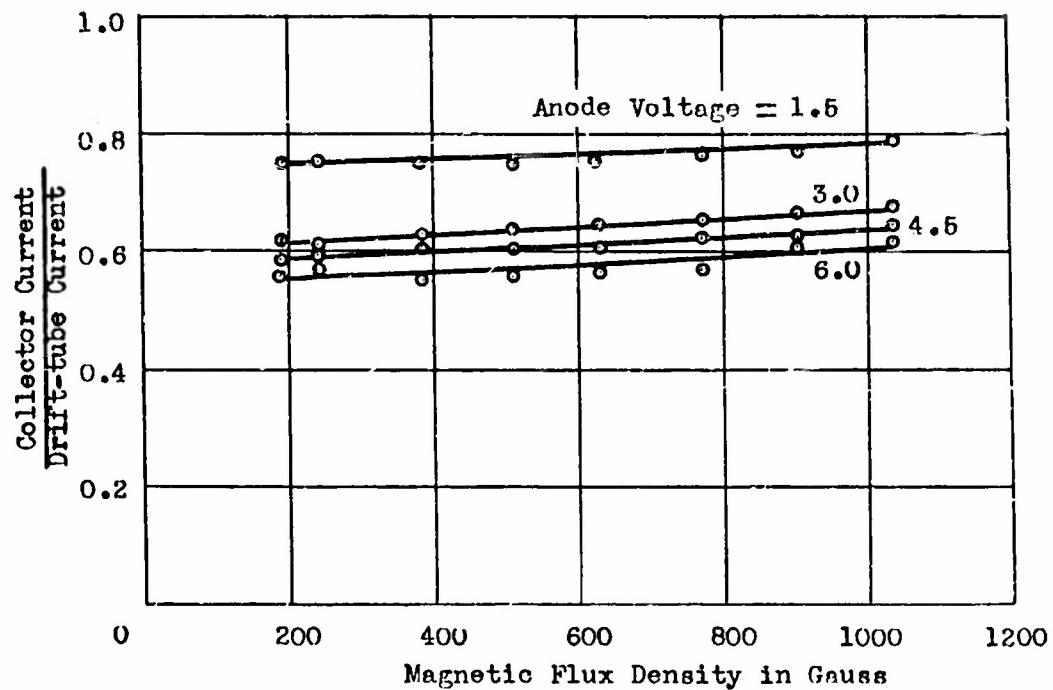


Fig. 3.5.--The effects of magnetic flux density and anode voltage on the fraction of drift-tube current passed by the detector grid.

CHAPTER IV

MEASUREMENT OF NOISE IN BEAM CURRENT

Evaluation of inherent noise in the tube currents is performed by comparing the tube noise with the noise from a temperature limited diode.

A low noise preamplifier with a voltage gain of 50 was constructed to work in cascade with a Hewlett-Packard Model 450A amplifier. The schematic for the preamplifier is shown in figure 4.1¹. The grounded-cathode-grounded-grid sequence was used to obtain a low noise figure². The equivalent noise resistance in the input grid circuit is 1500 ohms. The overall voltage gain of the two amplifiers is 5000 which is sufficient to allow measurement of the noise level in the input resistor alone. The entire amplifier is thoroughly shielded, and the preamplifier is supplied with DC heater current and a highly regulated plate supply. The lower end of the 3db pass band was set at 15 KC by means of an R-C filter on the output so that power frequencies and other low frequency disturbances could be eliminated.

¹RCA Tube Handbook, Vol. 5-6, Circuits for 6 BQ7 tube.

²G. E. Valley and H. Wallman, Vacuum Tube Amplifiers, (New York: McGraw-Hill Book Co., Inc., 1948), Chapters 13, 14.

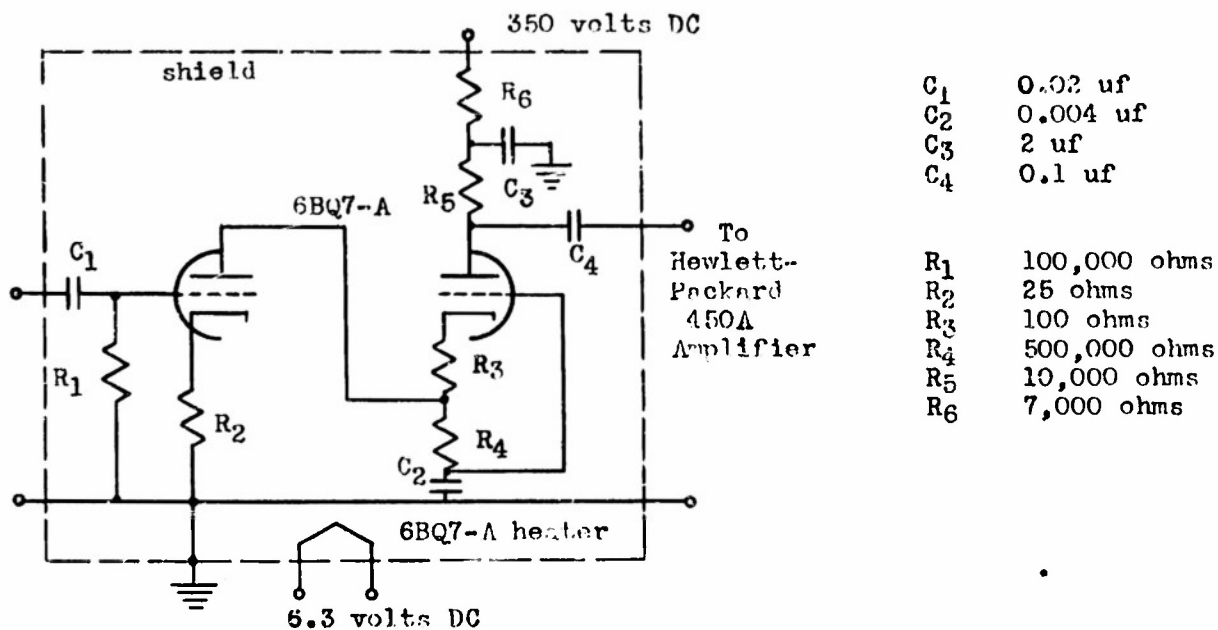


Fig. 4.1.--Schematic diagram for low-noise preamplifier.

Measurements are made by comparing the noise produced by the tube under test to the noise alternately fed into the same amplifier by a temperature limited diode with a tungsten filament. The noise from this latter tube is easily calculated from the well-known formula for shot noise,

$$\bar{i}^2 = 2eI_pB \quad (4-1)$$

where \bar{i} is the rms noise current, e is the charge on an electron, I_p is the temperature limited DC plate current of the noise tube in amperes, and B is the bandwidth in cycles per second.

Both the beam tester tube and the diode noise tube constitute constant current generators. Therefore, input capacitance to the amplifier and the input resistor size both influence bandwidth of the noise appreciably. Both the beam tester tube and the noise diode are kept connected to the amplifier, so that no change in input shunting capacitance (and thus, bandwidth) can occur. First, the beam tube is adjusted as desired and the resultant noise output from the amplifier noted on a voltmeter with square law response to the noise. Then the beam tube is shut off, and the noise diode filament is heated until the amplifier output is duplicated. This is a valid operation because both sources generate white noise in the bandwidth considered (barring oscillations which will be treated below). A reading of the diode plate current completes the measurement.

Noise measurements have only recently been started, and only collector current noise has been dealt with so far. Initial results are as follows:

1. Noise "peaks" several times the minimum observed noise level have been detected as anode voltage is varied. Similar peaks are observed as magnet current is varied.
2. Sinusoidal oscillation at frequencies from 400 kc to 2 mc were noted in the beam tube collector current at 1.8 anode volts. Amplitude of the oscillation ranges up to ten or more times the beam noise. Frequency was affected by a slight change of either anode or grid voltage. These oscillations have been observed in the past in cyclotron-mode tubes, and subsequent experiments will attempt to explain their origin and behavior.

3. In those regions where oscillation and noise peaks were absent, the noise in the collector current closely agreed with that which would be found in an equal DC anode current in a temperature-limited diode. It appears that the collector draws over all the current from a virtual cathode in the vicinity of the grid. Indeed, the current versus voltage characteristics of the collector would lend support to this view. A parallel experiment with a conventional pentode will be performed as a check.

Partition noise and collector noise with the collector and grid at other than voltage-saturated bias levels will be measured next.

The above represents only preliminary results and observations. It is intended that complete results of the noise measurements will be available for the next report.

CHAPTER V

CALCULATION OF DETECTING GRID CHARACTERISTICS

Any consideration of the means by which a grid is able to detect changes in radii of electron paths is complicated by the fact that we must deal with a distribution of initial velocities, rather than a perfectly homogeneous electron beam. Under the influence of a radio-frequency electric field, the radius of an individual electron path may either increase, or decrease, or remain unchanged, depending upon the relative phase of the electron and the r-f signal. Thus the effect of the r-f field is to alter the distribution of radii. For weak signals, the change in distribution is slight, while for strong signals, we would expect that all electrons in the beam would be "pulled into step" with the r-f signal. We shall deal only with signal case.

This report will include an outline of the method of analysis, and a brief summary of results. A full report on this subject is to be issued in the near future.

The object of the analysis is to determine amplitude and frequency response for deep "honeycomb" grid structures with various hole sizes, in an effort to determine the optimum grid size.

5.1 Outline of Solution for the Quiescent Condition

It is assumed that electrons enter the interaction region with the distribution of transverse velocities that would prevail at the cathode, given by

$$f(v_t) = A v_t \cdot e^{-\frac{m}{2KT} v_t^2} \quad (5-1)$$

where m is the electron mass, K is Boltzman's constant, T is the cathode temperature in degrees Kelvin, and v_t is transverse velocity, all in MKS units.

If we arbitrarily choose the constant A such that

$$\int_0^{\infty} f(v_t) dv_t = 1 \quad (5-2)$$

then $A = \frac{m}{KT}$, and equation (5-1) becomes

$$f(v_t) = \frac{m v_t}{KT} \cdot e^{-\frac{m}{2KT} v_t^2} \quad (5-3)$$

The above choice of the constant A is equivalent to saying that the total current is unity.

It is more convenient to write the equations in terms of radius of the helical electron path. This is readily done if we note that $v_t = \omega_0 r_0$, when $\omega_0 = 2\pi f_0$, and f_0 is the cyclotron frequency defined by equation (1-1) and r_0 is the radius of the path.

We can now write, with the requirement that

$$\int_0^{\infty} g(r_0) dr_0 = 1,$$

a new distribution function

$$g(r_0) = \frac{m \omega_0^2 r_0}{KT} \cdot e^{-\frac{m \omega_0^2 r_0^2}{2KT}} \quad (5-4)$$

We are interested first in the fraction of the total current that will be intercepted by a grid under the no-signal condition. The assumption is made that an electron, whose path has a radius r_1 , will be captured by the grid if the axis of the path lies within a distance r_1 of one of the vanes of the grid. (It is also assumed that the pitch of the electron path is less than the depth of the grid.) For the purpose of a numerical analysis, we divide the grid opening into n regions spaced at different distances from the walls, each region having some area A_1 , which is a fraction $\frac{A_1}{A_t}$ of the total area of the opening. If we consider the total current approaching the grid openings to be unity, the current captured by the grid will be

$$I_g = \sum_{i=1}^n \frac{A_1}{A_t} e^{-\frac{m\omega_0^2 r_1^2}{2KT}} \quad (5-5)$$

The above expression does not include current captured because of the finite grid area, which is about 15 percent of the total area for the practical grids that have been used. Thus the total beam current is greater than unity, and is given by

$$I_o = 1 + \frac{.15}{1-.15} \quad (5-6)$$

The collector current is, of course, total beam current minus the grid current.

5.2 Experimental Results for the Quiescent Case

It is interesting to compare the results of the previous section with data obtained from the beam tester tube. By merely varying the magnetic field strength, we can change the scale of abscissa on the

initial radius distribution curve, thus shifting the curve to right or left. The rate of change of the current division factor ($\frac{I_{coll}}{I_0}$) with respect to flux density is a measure of the sensitivity of the grid as a detector. Also, this affords a means of checking our analysis. Figure 5.1 shows the measured and calculated characteristics for two different accelerating voltages. Note that for low magnetic field strength the error is very large. This is probably because we have violated the assumption that the pitch of the electron path is less than the grid depth.

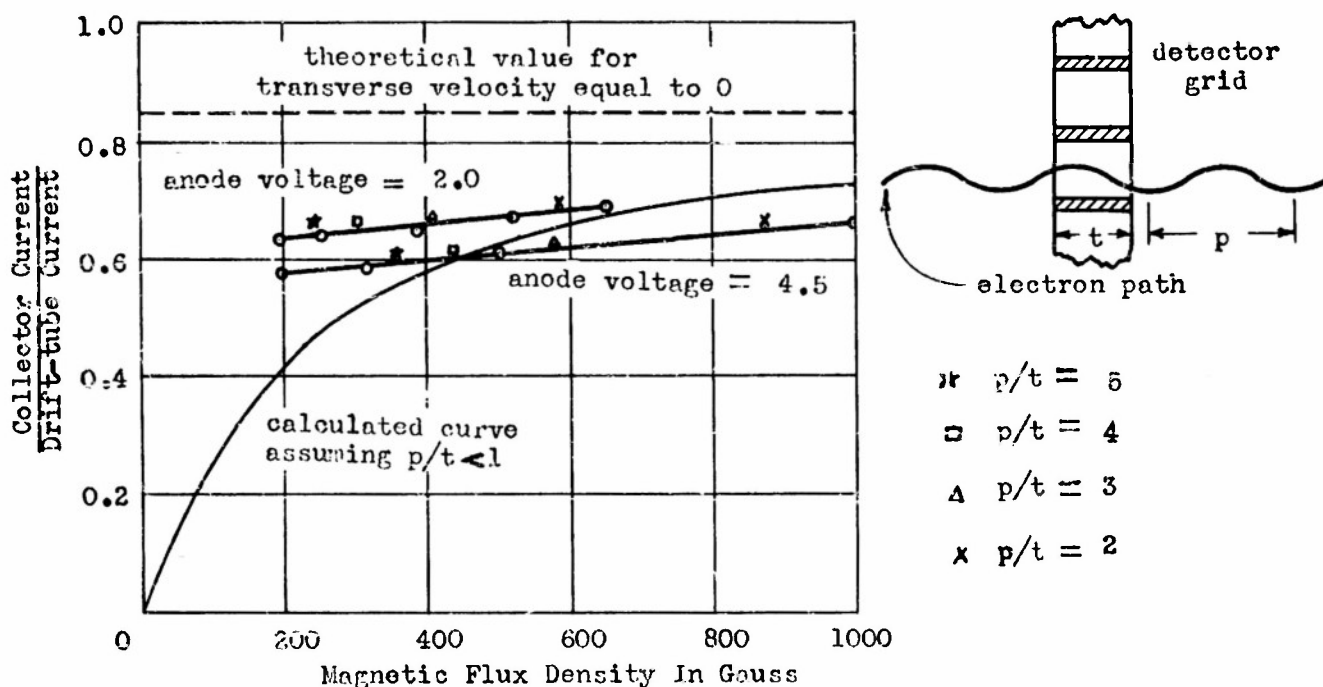


Fig. 5.1.

At high flux densities, collector current is lower than the calculated value. This may be the result of transverse velocities imparted to the electrons as they pass near the wires of the accelerating grid. Future tests will prove or disprove this idea,

but at least it is substantiated by the fact that reduced anode voltages give very nearly the predicted current division (cf. Fig. 5.1).

5.3 The Small Signal Case

We consider r-f power input to the tube to be small when the changes in radius produced by interaction of electrons with the r-f field are comparable to the initial radii of the electron paths. There is a change in the distribution function for the radii, but the electrons are not all "pulled into step" with the r-f field.

Analysis of this case is not simple, but a numerical solution has been obtained.

The method for solving this problem follows. Knowing the current reaching the collector under quiescent conditions, we seek the change in current under signal conditions.

A finite number of categories are established, each containing electrons whose paths have nearly the same radius. A second division is made to group electrons having about the same phase with respect to the r-f field. This amounts to treating the beam as if it were made up of a relatively small number of charges, each having a particular phase and a definite initial radius. The effect of the r-f field on each of these charges can be calculated, and the net change in grid or collector current can then be computed.

The details of the above process are quite involved and will be left to a technical report on that subject; but the important conclusions can be stated rather simply in terms of curves of changes in collector current as a function of r-f power input. It is necessary, of course, to specify the form of the interaction structures, and the accelerating voltage, as well as the configuration of

the grid. Cathode temperature is also specified, although variations within a reasonable range of operating temperatures have little effect on the solution.

The curves of figure 5.2 show the changes in collector current as a function of the r-f power input. The interaction structure chosen for these calculations was a waveguide $1/8$ inch high and 3 inches wide, while the detector was a deep "honeycomb" grid with square holes of the sizes specified on the curves, and with a depth greater than the pitch of the electron paths. The electron velocity corresponds to an accelerating voltage of one volt, and cathode temperature was assumed to be 850°C . The calculations were made for a resonant frequency of 3000 megacycles per second.

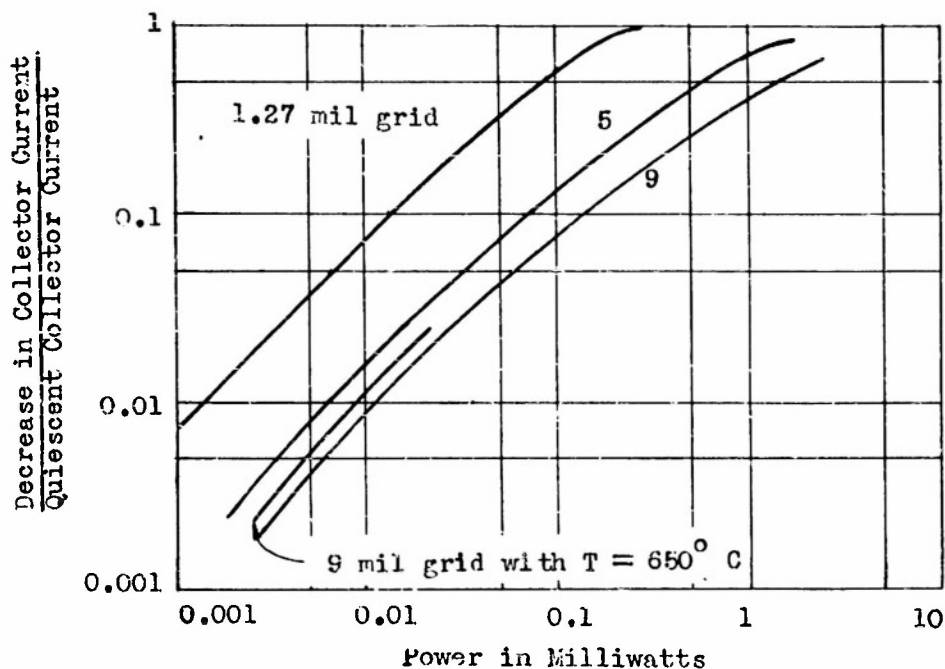


Figure 5.2

It appears from the curves that the smaller the grid openings the better. However, we must consider also the fact that the current transmitted to the collector under quiescent conditions decreases as the grid is made smaller, and that the actual signal is proportional to the total current. By combining these facts, we should be able to arrive at an optimum grid size.

We will assume for this discussion that the grids have square holes with 85 percent transmission of light, regardless of the size of the holes. Thus 15 percent of the beam current is captured because of finite thickness of the vanes. The remaining current - that directed at the holes - we will call I_1 , the active beam current.

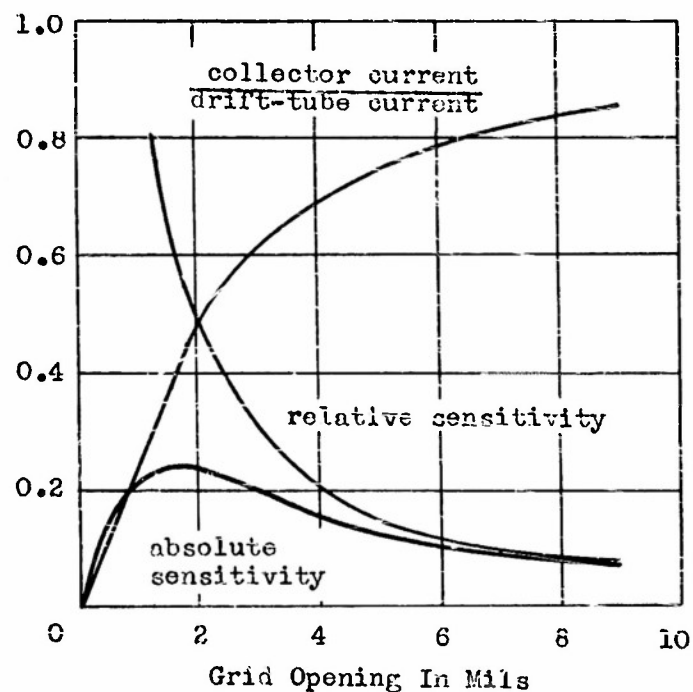


Figure 5.3

Relative sensitivities for grids of different sizes can be taken from figure 5.2 in the region of linear characteristics, using any fixed value of r-f power.

The ratio of quiescent collector current to beam current for any grid size can be calculated by the method of section 5.1.

The product of the above quantities of the absolute sensitivity of the grid structure; i.e., it is proportional to the actual signal current at the collector. This product is plotted in figure 5.3, and gives the important result that the maximum sensitivity to be expected from this type of grid structure is about 5 or 6 db better than has actually been obtained with Varian klystron grids (.011 inch openings) and would be obtained with grid openings of about .002 inches. This may or may not be a practical grid from the standpoint of manufacture.

It is also important to note that the grids all tend to saturate at high power levels, and less power is required to saturate smaller grids. The dynamic range is probably almost independent of hole size.

DISTRIBUTION LIST

Nonr 1147(01)			NR 073-571		
Addressee	Attn	No. of Copies	Addressee	Attn	No. of Copies
Chief of Naval Research Department of the Navy Washington 25, D.C.	Code 427	2	Commanding General Wright Air Development Center Wright-Patterson Air Force Base, Ohio		1
Director Naval Research Laboratory Washington 25, D.C.	Code 3940 3470 2000	1 1 6	Commanding General Air Research & Development Command Post Office Box 1395 Baltimore 3, Maryland		1
Chief, Bureau of Ships Navy Department Washington 25, D.C.	Code 840 816	1 1	Commanding General Air Force Cambridge Research Center 230 Albany Street Cambridge 39, Massachusetts		1
Chief, Bureau of Aeronautics Navy Department Washington 25, D.C.	EL 45	1	Chairman Panel on Electron Tubes 346 Broadway 10th Floor New York, New York		1
Chief, Bureau of Ordnance Navy Department Washington 25, D.C.	Re9d	1	Armed Services Technical Information Agency Document Service Center Knott Building Dayton 2, Ohio		5
Commanding Officer Office of Naval Research Branch Office 1000 Geary Street San Francisco 9, California		1	Office of Technical Services Department of Commerce Washington 25, D.C.		1
Commanding Officer Office of Naval Research Branch Office John Crerar Library Building 86 E Randolph Street Chicago 1, Illinois		2	Bell Telephone Laboratories Murray Hill Laboratory Murray Hill, New Jersey	Dr. J.R. Pierce	1
Commanding Officer Office of Naval Research Branch Office 346 Broadway New York 13, New York		1	California Institute of Technology Department of Electrical Engineering Pasadena, California	Dr. L.M. Field	1
Commanding Officer Office of Naval Research Navy #100 Fleet Post Office New York, New York		2	Harvard University Division of Applied Science Cruft Laboratory Cambridge 38, Massachusetts		1
Chief of Naval Operations Navy Department Washington 25, D.C.	Op 423	1	Hughes Aircraft Co. Research and Development Culver City, California	Dr. A.V. Haefl, 1 Electron Tube Research Laboratory	
Director Signal Corps Engineering Laboratories Evans Signal Laboratory Supply Receiving Section Building #42 Belmar, New Jersey	Thermionics Branch Countermeasures Branch	1 1	University of Illinois Electronics Engineering Department Urbana, Illinois	Prof. H.M. von Foerster	1
Commanding General Rome Air Development Center Griffiss Air Force Base Rome, New York		1	Massachusetts Institute of Technology Research Laboratory of Electronics Cambridge 39, Massachusetts	L. Smullin	1
			Stanford University Electronics Research Laboratory Stanford, California		1